GEOSCIENCE Australia

Record 2001/45

Hamersley Province Seismic Survey 1997: Processing Report

L.E.A. Jones and B.R. Goleby

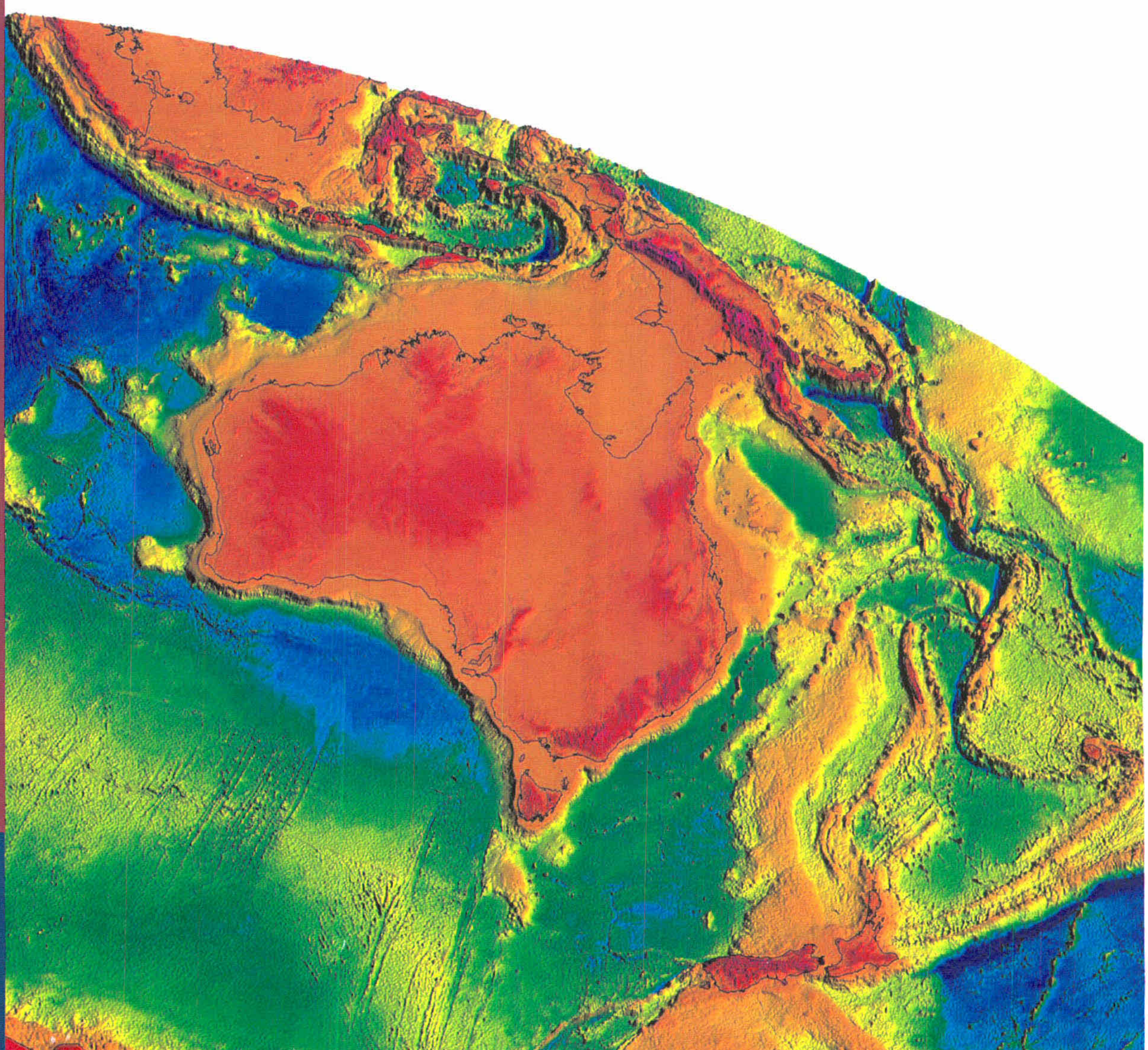

SPATIAL INFORMATION FOR THE NATION

GEOSCIENCE
AUSTRALIA

Hamersley Province Seismic Survey 1997: Processing Report.

Geoscience Australia

RECORD 2001/45

by

L.E.A. Jones and B.R. Goleby

Geoscience Australia, GPO Box 378, Canberra, ACT, 2601.

GEOSCIENCE AUSTRALIA

Geoscience Australia

Chief Executive Officer: Dr Neil Williams

ISSN 1039-0073
ISBN 0 642 467269

Bibliographic Reference: Jones, L.E.A. and Goleby, B.R., 2001. Hamersley Province Seismic Survey 1997: Processing Report. Geoscience Australia, Record 2001/45, 24pp.

TABLE OF CONTENTS

ABSTRACT

In 1997, the Australian Geological Survey Organisation, now Geoscience Australia (GA), the Tectonics Special Research Centre (TSRC), MERIWA (Minerals and Energy Research Institute of WA), BHP Iron Ore Pty Ltd and Robe River Pty Ltd undertook a joint deep seismic research project. This project was aimed at imaging the crustal setting of the Hamersley Province region to refine the knowledge of the structure, tectonics, and fluid migration pathways. The project's objectives were to obtain a better understanding of the sub-surface geology of the Hamersley Province at both a regional scale and mine scale.

The Hamersley Province Survey Seismic Survey (GA Seismic Survey L144) was undertaken from July to August in 1997. 136 km of nominally 10 fold CMP (common midpoint) deep reflection seismic data were acquired along two traverses. The three lines, 97AGS-HB1, 97AGS-HB2 and 97AGS-HB3 constituted the Hamersley Basin Traverse, while line 97AGS-SD1 made up the Sylvania Dome Traverse.

This record describes the processing methodology applied to the data to produce the final stack sections and migrated stacks used in the interpretation. A major problem encountered during acquisition was the loss of seismic energy due to the nature and thickness of the regolith, and absorption with particular geological formations such as the cavernous Marra Mamba Formation. A particular aim of the seismic processing therefore was the recovering and enhancing of the seismic signal recorded in the field.

Key processing steps included crooked line geometry definition, spectral equalisation and filtering, calculation of static corrections, velocity analysis and coherency enhancement. Spectral equalisation was successful in extracting signal from noise in those areas with appreciable signal, i.e. where reflected energy could just be observed on the shot records. Determination of refraction statics corrections revealed a considerably variable regolith with thickness up to several hundred metres in places. Both refraction statics and automatic residual statics however did not bring about significant improvement in the stack in the poor data areas. The windows of good data were dependent upon the regolith and sub-surface geology, occurring where the regolith is thinner, usually within a dolerite unit of the Fortescue Group.

Although the resolution of seismic data was generally not good, some significant details are shown within areas of the Hamersley Province which provide sufficient information for the development of a crustal structure model.

1. INTRODUCTION

The Hamersley Province Seismic Survey (GA Seismic Survey L144) was undertaken in July to August 1997 as a joint investigation between AGSO, the Tectonics Special Research Group of the University of Western Australia, Curtin University, and mining companies BHP Iron and Robe River. The overall goal of the survey was a detailed deep seismic image to assist in understanding the structure and history of one of the world's best-exposed Palaeoproterozoic fold and thrust belts, the location of a major iron-ore mining province.

The survey consisted of four lines: 97AGS-HB1, 97AGS-HB2 and 97AGS-HB3, which constituted the Hamersley Basin Traverse, and 97AGS-SD1, the Sylvania Dome Traverse, as shown in Figure 1. The seismic data was acquired by GA's Land Seismic Group, using the facilities of Australia's National Seismic Imaging Resource (ANSIR), and processed in-house at AGSO using Paradigm's Disco/Focus seismic processing package. One of the challenges for data processors was the variable quality of seismic data along the lines, due principally to the nature of the regolith.

2. SUMMARY OF ACQUISITION

For all lines, a nominal split-spread geometry was employed, except at the ends of the lines where the shot was "walked" on (/off) the spread at the first (/final) location. Each receiver group comprised 16 in-line geophones at a 2.5 m spacing. Seismic channel #1 corresponded to the first group (at the northern end of the spread), seismic channel #120 to the last group, while the shot was nominally at seismic channel #61. The geometry parameters for the four lines are summarised in Table 1. Details of the survey operations and data acquisition are covered at length in Goleby et al. (2001).

Field data was recorded on 9-track tape (SEG-D 6250 bpi) and exabyte (SEG-Y TAR 8500) as 20 second records (actually 10240 samples @ 2 milliseconds). The shot records (120 channel; 20 s @ 2 ms) were read from the exabyte tapes and stored on temporary 3480 tapes for the duration of processing. These 3480 tapes were subsequently read, resampled to 4 ms and stored on disk.

3. PROCESSING

Production processing was carried out using Disco, while the interactive version Focus was used for parameter tests, first break picking and data quality control (QC), and stacking velocity estimation. The processing stream for 5 second data is shown in the text box below. Essentially, the same processing was used for the 20 second data, except that time varying parameters, including band pass filters, were modified. The final version was arrived at after numerous tests, principally on Line 97AGS-HB3. Other (rejected) processing streams differed in the order of application of steps, as well as in the type of processing modules employed. For example, several of the processing sequences involved F-K filtering on shots, but did not prove successful, due to crooked line acquisition and variable regolith. Details of processing tests and the chosen parameters are discussed below.

```
(1) DEMULTIPLEX: SEG-D TO SEG-Y (&
DISCO INTERNAL) USING FIELD EAVES-
DROPPER SYSTEM

(2) GEOMETRY DEFINITION

(3) QUALITY CONTROL DISPLAYS & EDITS
& 75 HZ NOTCH FILTERING

(4) RESAMPLE DATA TO 4 MS

(5) SPHERICAL DIVERGENCE CORRECTION
C=1.0, V=2.0, T=1.0 WITH
VELOCITY FUNCTION = 5000-6500 M/SEC

(6) SPECTRAL EQUALISATION
GATES: (8/12-16/20) HZ X 8
OUTPUT WEIGHTS: 0/0, 8/0.5, 16/1,
24/1.5, 40/2, 4/1.5, 72/0.5, 100/0

(7) BANDPASS FILTER
TIME(S) FREQ(HZ)/SLOPE(DB/OCTAVE)
0 - 5 S  24/36 - 72/36

(8) FRONT END MUTE APPLIED,
HANDPICKED FOR EACH SHOT

(9) STATIC CORRECTIONS APPLIED
REFRACTION STATICS - SINGLE REFRACTOR
AUTOSTATICS (WITH STRUCTURE)

(10) SHOT BALANCE, GATE: 1.0 - 3.5 S

(11) NORMAL MOVEOUT CORRECTION
20 % STRETCH MUTE APPLIED

(12) COHERENCY ENHANCEMENT - SHOTS

(13) CDP SORT (TO CROOKED LINE)

(14) MEDIAN STACK

(15) SECTION BALANCE
GATES 0.5 - 1.5 S, 2 - 3.5 S

(16) COHERENCY ENHANCEMENT - CDP
SECTION

(17) AGC - 500 MS GATE

(18) DISPLAY OF PROCESSED DATA
```

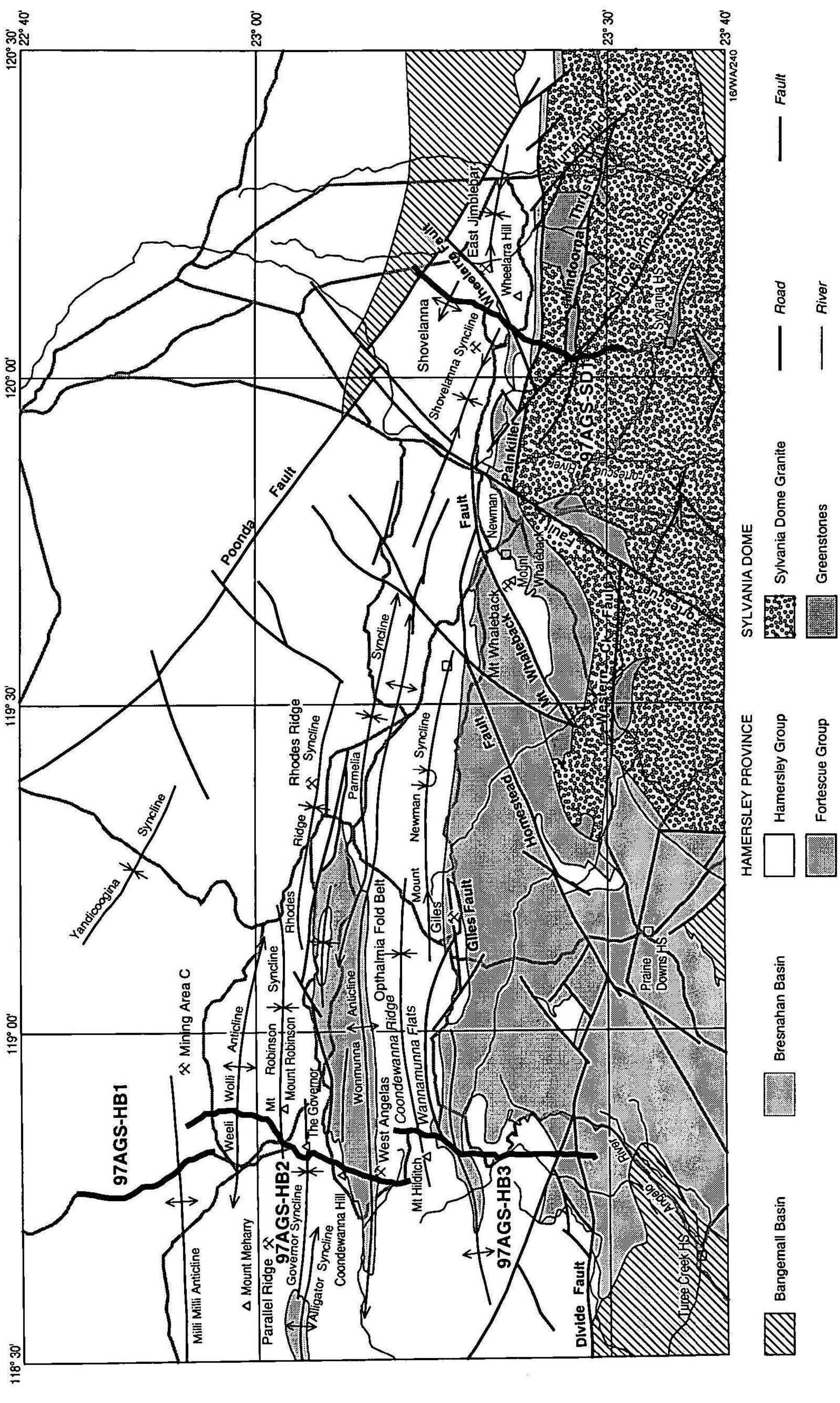

Figure 1: Simplified geological map of the Hamersley Basin / Province, showing location of the Hamersley Deep Seismic Lines.

3.1 Geometry

The Disco/Focus LINE, PATTERN and SOURCE modules were employed to calculate and enter the geometry into the Disco seismic database. Table 1 provides a summary of the line geometry. The X and Y coordinates, and elevation of each station as surveyed were input via LINE. In order to associate each channel of each shot record with a receiver station, it was necessary to define first appropriate patterns for the spread via PATTERN and then to run the SOURCE module. Within the SOURCE module, the following parameters are assigned for each shot: shot station, in-line and perpendicular offset of the shot from the station, pattern name and pattern origin location.

The geometry was checked by plotting shot and receiver location along with the midpoint of every shot-receiver pair. The crooked common depth point (CDP) line was defined to be a piecewise linear fit to the areal distribution of shot-receiver midpoints, with the constraint that the CDP numbers at bendpoints were twice the nearest station number. The CDP number and the corresponding X and Y coordinates were input via another call to LINE. A call to PROFILE prior to any actual seismic processing wrote/updated geometry information from the seismic database to the seismic trace headers and assigned each trace to a CDP. The maximum in-line and perpendicular distances beyond which a trace would not be assigned to a CDP was 80 m and 240 m respectively. Such traces would later be excluded by the CDP sort. This decision was based on comparison with tests in which all traces were assigned to a CDP.

3.2 Editing

The observer's logs and tape logs were used to identify shot records of dubious quality. The shot record field monitors were likewise examined. For shot misfires, the amplitude of all the traces in the shot record was set to zero via EDIT. End-mutes were applied on records that were shorter than full length to avoid possible contamination by spikes. A summary of edits is given in Table 2. Most of the mutes commenced at times greater than 5 s, with the exception of those for shots 26, 130 and 139 for Line 97AGS-SD1.

3.3 Notch filtering

In order to remove mechanical noise from the recording cab power generator, a 75 Hz notch filter (FILTER with NOTCH option) was applied for the three receiver stations centred on the recording cab position, as listed in Table 3. 50 Hz noise from electricity transmission lines was not a problem in the survey area.

3.4 Gain Correction

Corrections were made for amplitude loss with increasing time due to spherical divergence and intrinsic attenuation. The GAIN module was used with the SPHDIV option which uniformly multiplies all input traces with a time varying scalar of the form C * Velocity^V * Time^T. An average velocity function appropriate to the data was user supplied, namely 5000 m/s at 0 s to 6500 m/s at 5.5 s. The other parameters used were C=1, V=2 and T=1. Using a scalar of the form Velocity * Time equates to multiplying the amplitude of the trace by the radius of the spherical wavefront from the shot at the sample time, in other words compensating for the inverse-distance amplitude relationship of a spherical wave. Tests of parameters showed that better amplitude recovery at later times was obtained with Velocity^2. Thus the final parameters empirically corrected for other amplitude loss effects such as intrinsic attenuation.

3.5 Spectral equalisation and filtering

A key processing step aimed at improving the signal to noise ratio on the shot records was spectral equalisation. Spectral equalisation (SPEQ) employs a zero-phase deconvolution operator to perform spectrum balancing within the range of signal bandwidth. The balancing is performed by using a number of user-designed bandwidth's or frequency gates, with an option to specify the desired output spectrum. SPEQ is recommended for minimising contamination by noise generated near the surface, such as ground roll and airwaves.

Extensive tests of spectral equalisation parameters and subsequent band pass filter (FILTER with BP option) were carried out on selected shots for line 97AGS-HB3. "Before" and "after" comparisons were made for the seismic data (eg, Figures 2 and 3), and the corresponding frequency spectra (eg, Figure 4). The record for shot 88 located at station 3730 along line 97AGS-HB3 is a typical example of a shot record dominated by coherent trains of ground roll in the frequency range 10 to 20 Hz. There also appears to be other less-coherent, low frequency source-generated noise. Application of SPEQ successfully suppresses the low frequency noise such that latent reflections are revealed. The subsequent band pass filter removes residual trains of ground roll.

Table 1: Summary of Acquisition Parameters and Line Geometry for the Hamersley Province Seismic Survey.

LINE	97AGS-SD1	97AGS-HB1	97AGS-HB2	97AGS-HB3
AREA	Sylvania Dome	Marillana Ck – Area 'C'	Area 'C' – West Angelas	Coondawanda Ridge – Angelo R
# SHOTS	163	78	170	97
DIRECTION	N to S	N to S	N to S	N to S
LENGTH	38.84 km	23.20 km	41.16 km	32.80 km
STATIONS	1000 – 1971	1000 – 1580	2000 – 3029	3000 – 3820
CDP RANGE	2000 – 3942	2000 – 3160	4000 – 6058	6000 – 7640
GROUP INTERVAL	40 m	40 m	40 m	40 m
SP INTERVAL	240 m	320 m	240 m	320 m
# CHANNELS	120	120	120	120
FOLD (NOMINAL)	1000%	800%	1000%	800%

Table 2: Summary of Shot Record Edits.

LINE	"ZEROED" SHOTS	END-MUTED SHOTS
97AGS-SD1	9, 106, 161	3, 26, 99, 118, 130, 136, 139, 141, 155
97AGS-HB1	51, 52, 66, 70	43
97AGS-HB2	40	31, 68
97AGS-HB3	3, 14, 22, 73	60

Table 3: Summary of 75 Hz Notch Filter Application.

LINE	RECORDING CAB POSITION (STATION)
97AGS-SD1	1080, 1242, 1379, 1460, 1625, 1729, 1838, 1855
97AGS-HB1	1120, 1252, 1418, 1501
97AGS-HB2	2092, 2190, 2265, 2348, 2468, 2628, 2783, 2872, 2940
97AGS-HB3	3150, 3178, 3288, 3406, 3582, 3654, 3713

Table 4: Summary of Refraction Statics Parameters (see 3.7 for a description of parameters).

LINE	97AGS-SD1	97AGS-HB1	97AGS-HB2	97AGS-HB3
X-cell (m)	80	80	80	80
Y-cell (m)	80	80	80	80
RADXY (m)	400	400	800	400
REPLVEL (m/s)	5600	5600	5600	5600
RADDT (m)	200	400	800	200
RADIV (m)	400	400	800	800
DATUM (m)	440	650	700	600

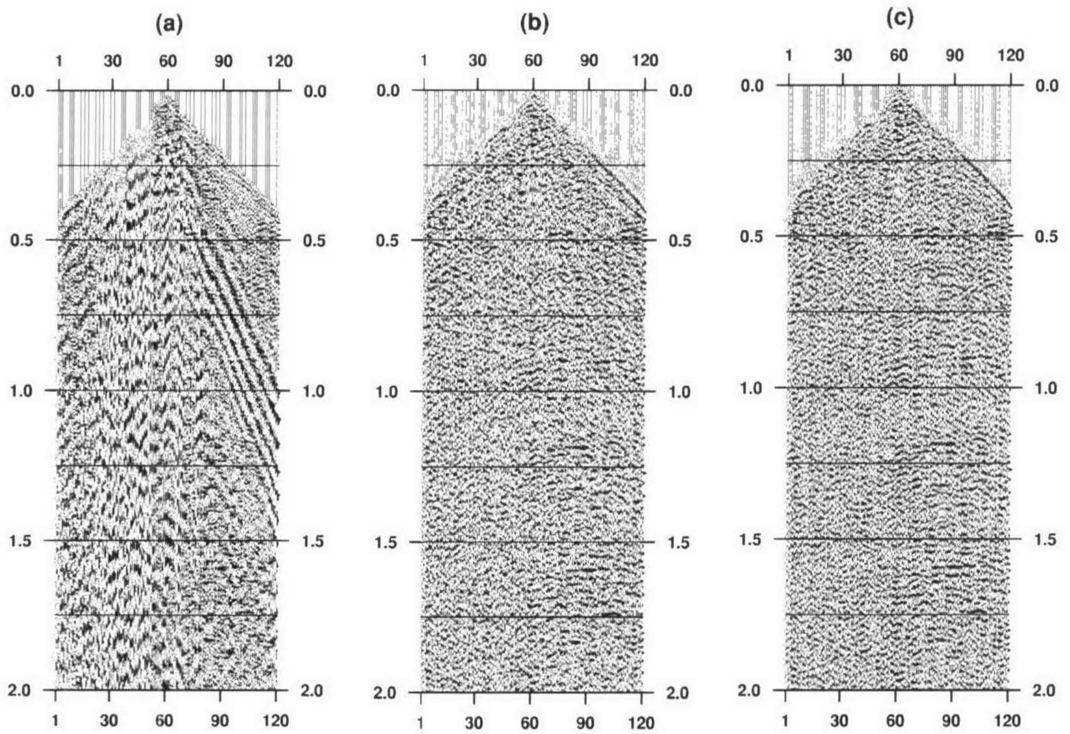

Figure 2. Shot record displayed to 2 s for Shot 88, Line 97AGS-HB3. (a) Prior to SPEQ (b) After SPEQ (c) After SPEQ and BP filter.

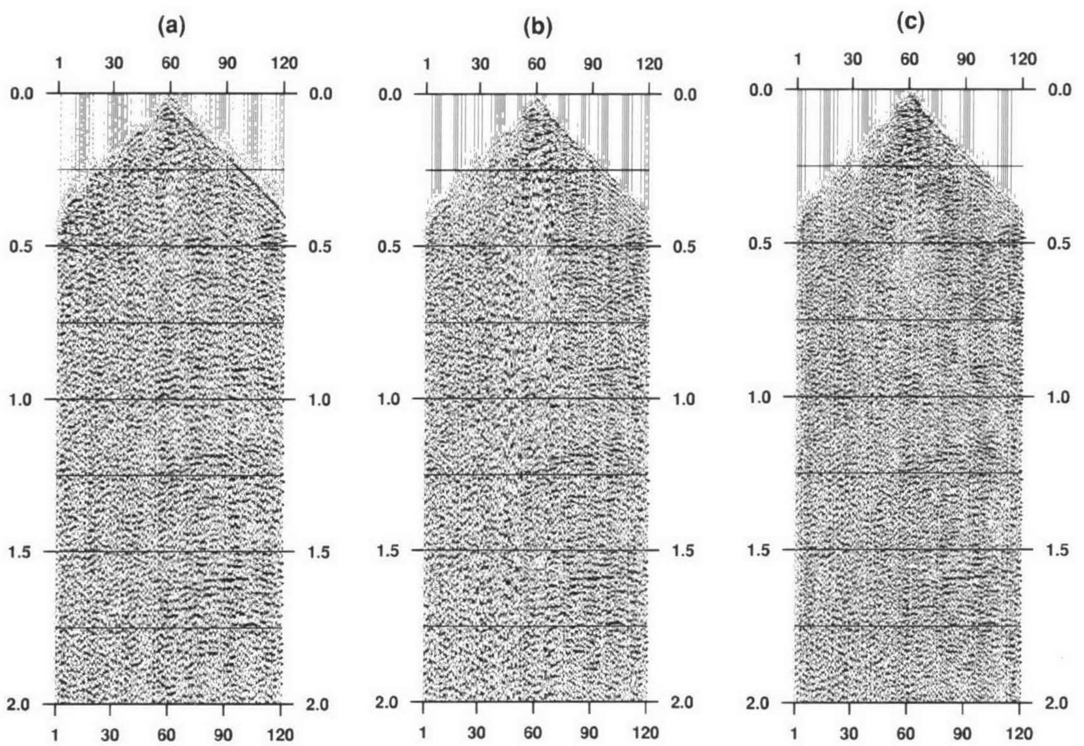

Figure 3. Shot record displayed to 2 s for Shot 88, Line 97AGS-HB3. (a) After final SPEQ and BP filter (Fig 2(c)) (b) After final BP filter only (24 Hz/36 dB/oct – 72 Hz/36 dB/oct) (c) After low-cut filter (32 Hz/48 dB/oct – 120 Hz/36 dB/oct).

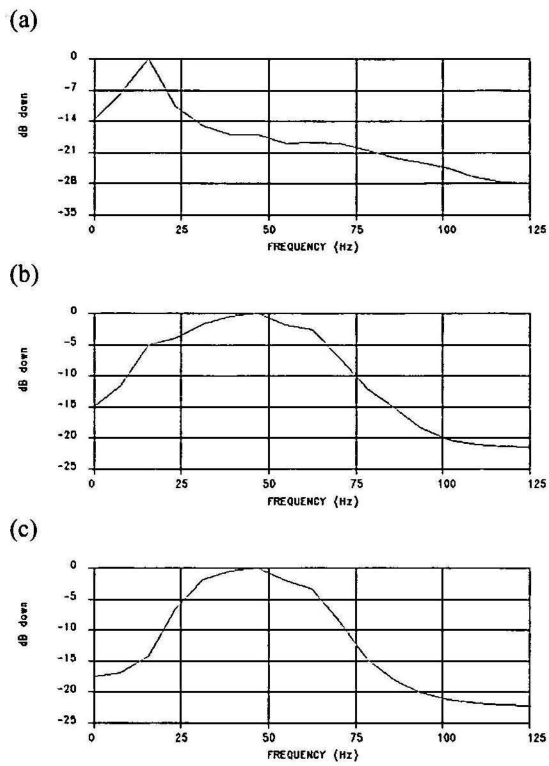

Figure 4. Frequency spectra for 0 – 2 s for Shot 88, Line 97AGS-HB3, corresponding to records in Figure 2. (a) Prior to SPEQ (b) After SPEQ (c) After SPEQ and BP filter.

Better results were obtained with many narrow contiguous design gates than with a few broad gates. Different designs for the shape of the desired output spectrum were also tested. The final parameters for spectral equalisation and following band pass filter are listed in the processing stream given earlier. The efficacy of these parameters is also demonstrated in Figures 2 and 4.

Spectral equalisation proved far superior to the use of a low-cut filter for the suppression of low frequency source generated noise. It was not possible to obtain equivalent results to the optimally designed spectral equalisation operator simply by using either the final band pass filter or a low cut filter, as shown by the comparisons in Figure 3.

3.6 Mutes

The application of SPEQ and BP filter also collapsed the reverberations in the first arrival wave train, thus reducing the severity of front-end mutes, which were picked interactively for all the shots. The mutes were saved as time-offset pairs defining a line across the shot record such that trace amplitudes at earlier times were set equal to zero. A stretch mute was also applied during normal moveout (NMO) correction but was not severe enough to remove all the first arrivals, only the parts of traces distorted by moveout correction. Although a more severe stretch mute could have substituted for the front-end mute, the philosophy here was that an individually tailored front-end mute was preferable given the low fold of the data and the highly variable terrain, weathering and geology along the lines.

3.7 Refraction Statics

First arrivals (first breaks) were picked on the first peak using the interactive FBNET module and automatically stored in the seismic database for use in the calculation of refraction statics. The stand alone executable FBSOL was used to monitor first break pick QC and for assigning the refractor segments, that is the range of offsets where the first arrivals corresponded to the refractor coinciding with the base of weathering. By experiment it was found that more stable solutions were obtained in the subsequent REFSOL module using a one-refractor model rather than a two-refractor model.

Inspection of the travel-time plots in FBSOL also suggested that a two-refractor model was not necessary in most cases. However, this assessment was difficult in areas with substantial lateral variation of refractor depth because the nominal split-spread geometry resulted in an asymmetric travel time plot, which was displayed only in terms of absolute value of offset in FBSOL. Nevertheless, the one-refractor model is believed to be satisfactory for the purpose of calculating statics since the major boundary between low velocity (average 2500 m/s) weathered material and high velocity (greater than 5000 m/s) bedrock is satisfactorily determined.

REFSOL calculates long wavelength statics due essentially to gradual changes in the topography of the surface, the base of weathering and short wavelength statics resulting from more rapid variations in topography as well as velocity variations in the weathered layer (Taner et al., 1998). How the statics are apportioned between the long wavelength and the short wavelength terms depends on smoothing parameters input to the program, as listed in Table 4, showing values of the parameters used for all four lines. RADXY is the radius for elevation smoothing. RADDT is the distance for smoothing of delay times and refractor velocities. RADIV is the interval velocity smoothing distance. REPLVEL is the replacement velocity. Velocity of weathering determined from uphole time and hole depth (variable but averaging around 1100 m/s for the Hamersley Basin lines and approximately 1300 m/s for the Sylvania Dome).

Interval velocities above the refractor and the offset range for the refractor were determined by inspection of the travel-time plots in FBSOL. As many values of offset range as were required to describe variations along the line were input. A constant value of 2500 m/s was used for the interval velocity above the refractor for all the lines. This was an average of values determined from the time-offset plots. The depth to the refractor and the calculated statics are sensitive to the choice of layer velocities above the refractor(s) and sensible values need to be estimated. It was found however that only small differences in statics resulted from using the constant value compared with variable layer velocities along the lines.

Various parameter tests were carried out and the program-estimated errors in the calculated shot and receiver statics were used as a guide in choosing optimum values. The effect of using a floating datum (surface elevation) was also investigated to allow later velocity analysis to be surface referenced. However no significant improvement in the quality of the stack was observed. The calculated statics were automatically stored in the seismic database. In addition, the refractor elevation, refractor velocity and delay time along the line were also calculated and stored, and proved useful not only in identifying possible faults, but also in explaining areas of poor reflection data quality.

The results of the refraction statics analysis presented in Figures 5 to 8 for the four lines demonstrate a significant statics problem in the survey area, not only in the magnitude of the one way (receiver) statics shown, but also in the variability along the line. Typically the values range from –20 ms to –100 ms, with some extreme excursions corresponding to deeply weathered areas. The short wavelength statics lie mostly within +/-10 ms for lines 97AGS-HB1, 97AGS-HB3 and 97AGS-SD1, and +/-15 ms for lines for line 97AGS-HB2. Both the long wavelength and short wavelength statics were applied to the data in the processing stream.

The refractor elevation and refractor velocity are also shown in these figures. Note that in many places there is a correspondence between low refractor elevation and low refractor velocity, with the most pronounced example occurring around station 3200 on line 97AGS-HB3 (Figure 7). This will be discussed further in the interpretation section. The depth of weathering can be seen more clearly in Figure 9 where refractor elevation and surface elevation are compared for all the lines. As will be seen later, there is a striking and not unreasonable inverse relationship between depth of weathering and seismic data quality, although the type of geology does also have an effect.

3.8 Automatic Statics

The automatic statics module STATICR was used in an attempt to fine-tune the quality of the stack in good data areas and to align any partially coherent events in the poor data areas. This operates on unstacked CDP gathers with NMO applied and essentially calculates the additional shifts (residual statics) necessary to maximise correlation of events across the gather in a selected time gate, such that shot and receiver consistency is maintained. The entire processing stream immediately prior to stack preceded the automatic statics routine with some additional mild coherency enhancement on the CDP gathers. In addition, more than one iteration was carried out in conjunction with stacking velocity analysis, using the autostatics to adjust events prior to an update of the velocity function which was then used in the next round of autostatics estimation.

To avoid forcing an interpretation through in the poor data areas, wide horizontal gates were designed and the residual structure option was employed. This procedure was satisfactory on the three Hamersley Basin lines with subhorizontal reflectors, but did not work on the southern end of 97AGS-SD1, where it was necessary to design dipping gates to remove structure.

A summary of the autostatics gate parameters is given below, where gate centres and widths are in ms. In each case, the maximum static shift was constrained to be 10 ms, less than half the dominant period of 20 to 25 ms.

97AGS-HB1

CDP	2000	2130	2300	2430	2431	3160
Centre	1160	1180	1270	1230	3500	3500
Width	400	400	400	400	1600	1600

97AGS-HB2

CDP	4000	6058
Centre	1300	1300
Width	1200	1200

97AGS-HB3

CDP	6000	7640
Centre	1200	1200
Width	1400	1400

97AGS-SD1

CDP	2000	3200	3201	3649	3650	3942
Centre	1200	1200	700	2050	600	2000
Width	1400	1400	800	800	800	800

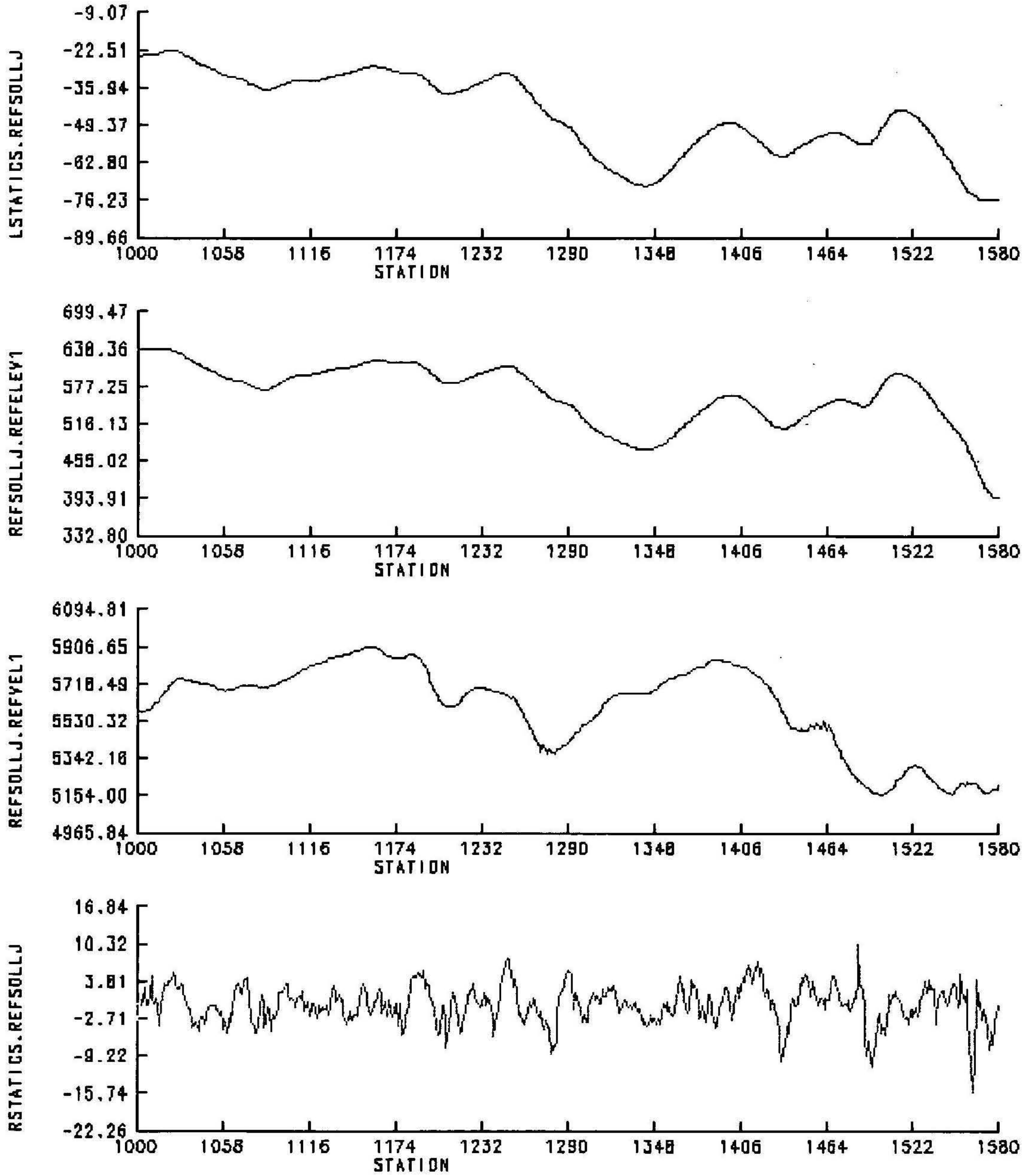

Figure 5. Refraction statics solutions for Line 97AGS-HB1. From top to bottom, long wavelength statics (ms), refractor elevation (m), refractor velocity (m/s) and short wavelength statics (ms) versus station. North is on the left.

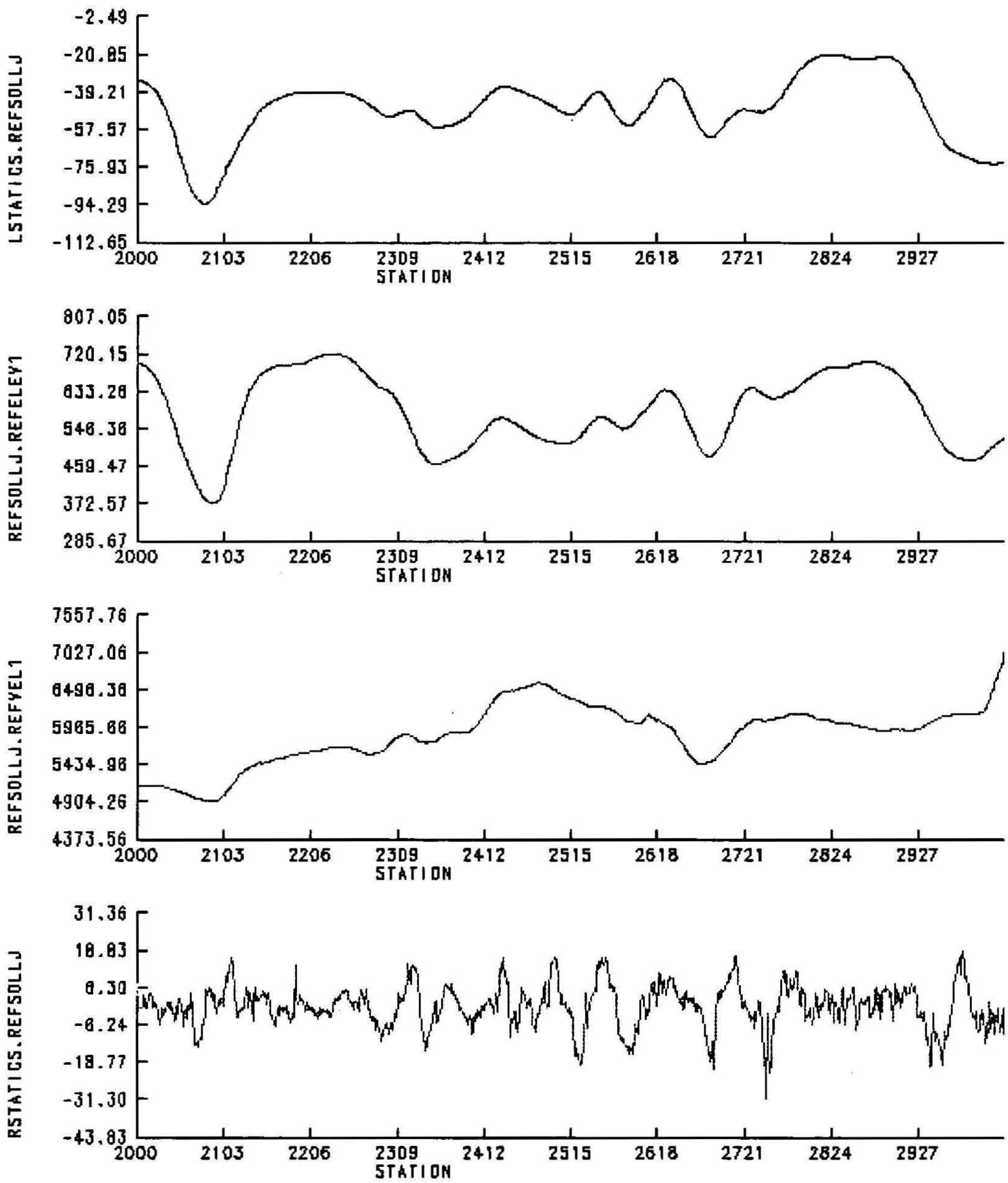

Figure 6. Refraction statics solutions for Line 97AGS-HB2. From top to bottom, long wavelength statics (ms), refractor elevation (m), refractor velocity (m/s) and short wavelength statics (ms) versus station. North is on the left.

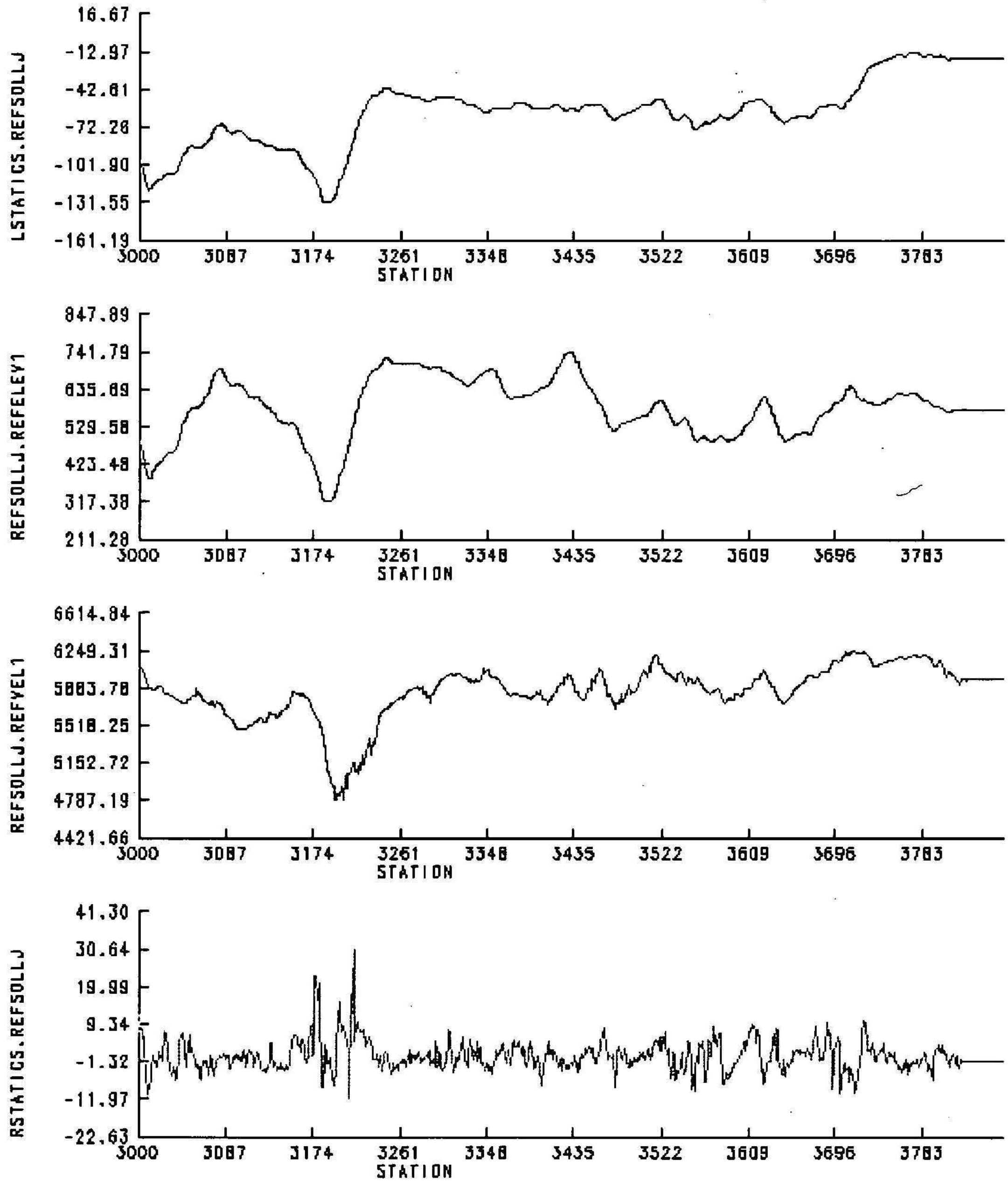

Figure 7. Refraction statics solutions for Line 97AGS-HB3. From top to bottom, long wavelength statics (ms), refractor elevation (m), refractor velocity (m/s) and short wavelength statics (ms) versus station. North is on the left.

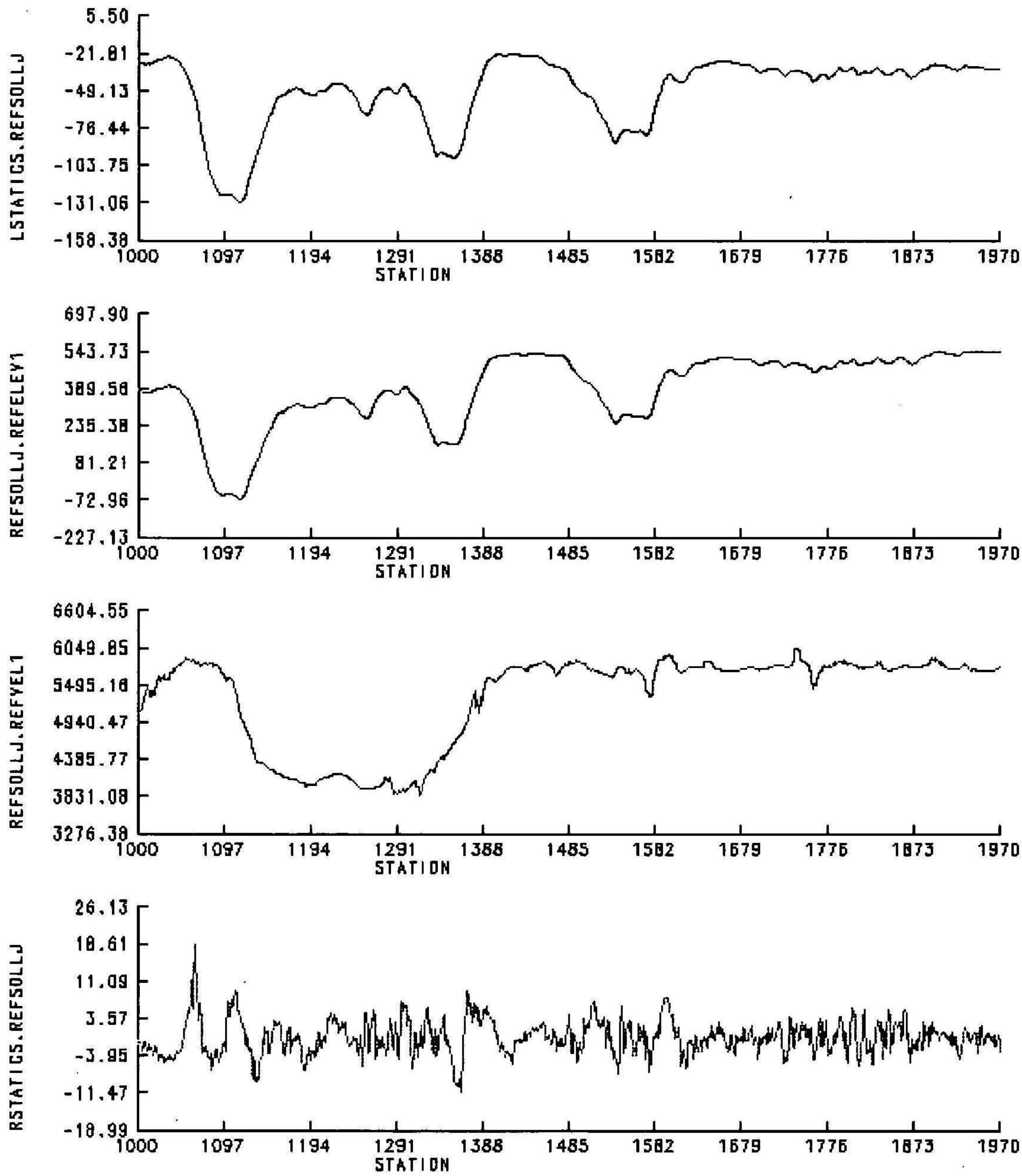

Figure 8. Refraction statics solutions for Line 97AGS-SD1. From top to bottom, long wavelength statics (ms), refractor elevation (m), refractor velocity (m/s) and short wavelength statics (ms) versus station. North is on the left.

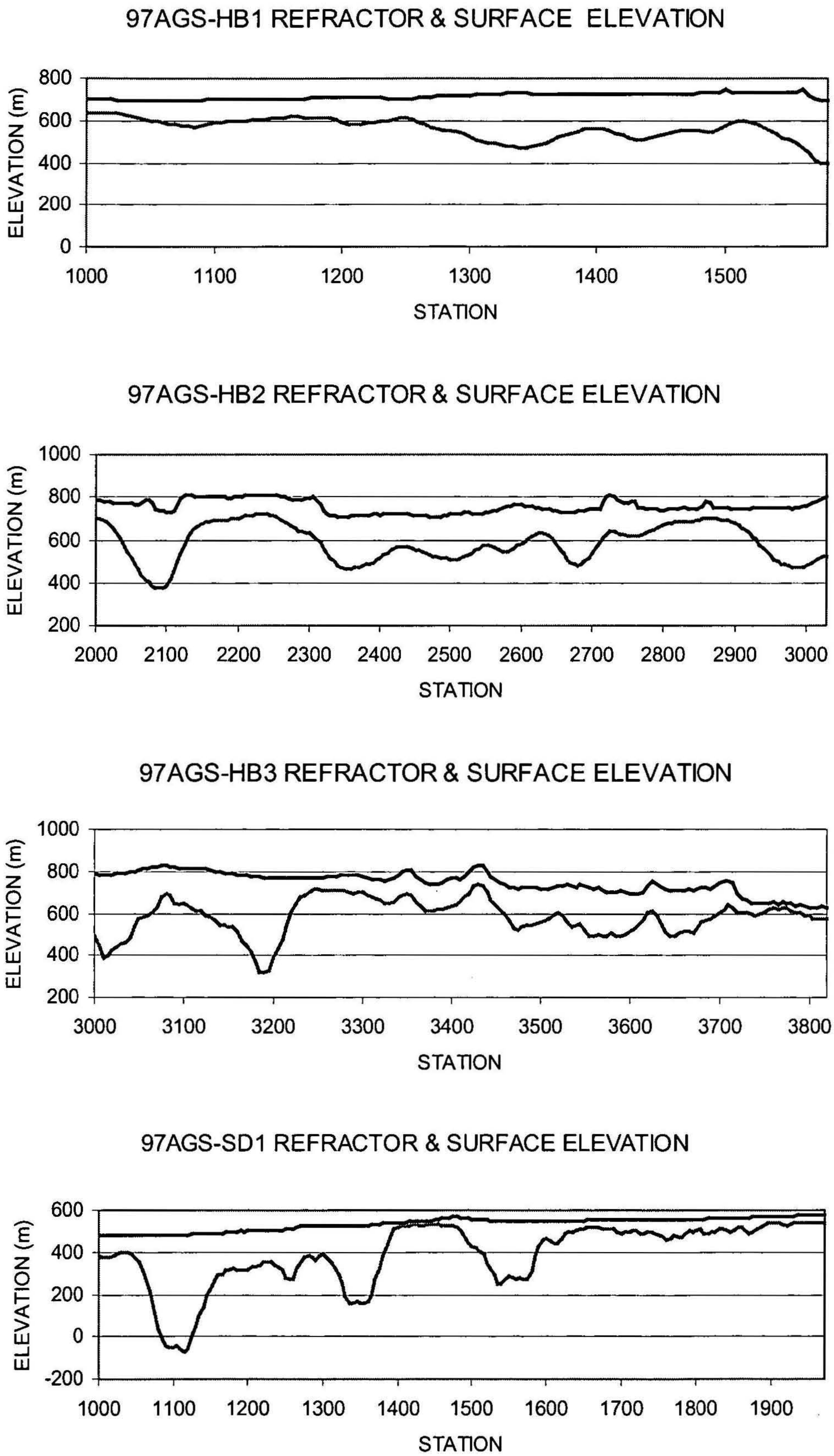

Figure 9. Composite display of refractor and surface elevation for each of the lines (from top to bottom) 97AGS-HB1, 97AGS-HB2, 97AGS-HB3 and 97AGS-SD1. North is on the left.

3.9 Velocity Analysis

Stacking (moveout) velocity is always critical in seismic processing. In hardrock areas, it is not as critical a parameter as in sedimentary basins because of the very fast velocities of the rocks encountered and hence the small moveouts recorded. In this study, it was found that the stack quality was sensitive to variations in stacking velocity in the top 2 s of data, particularly so in the upper 1 s. This conclusion was also borne out by calculating and plotting NMO hyperbola for a range of velocities and two-way travel times. These showed that at 1 s at the far offsets, NMO corrections would lie between 110 ms and 65 ms for velocities from 5000 to 6500 m/s, a correction range certainly greater than the dominant period.

Two different methodologies were used for determining stacking velocity. In both cases, the full processing stream preceded velocity analysis, including application of refraction statics and in following iterations, automatic statics. For line 97AGS-HB3 with lower fold, constant velocity analysis (CVA) was employed. Examination of stack panels produced for a number of CDP ranges with a range of stacking velocities led to the optimum choice. Note that in the range 0-1 s, the effect of +/-500 m/s was quite noticeable on the stack. The final choice using spatially varying velocity functions yielded significantly improved results over a single time varying velocity function.

For the other lines, the interactive Focus module VELDEF was used. To minimise the problem of low fold, three CDP gathers were combined into a super-gather. Velocity picks were made on the basis of maxima in coherency, aided by flattening across the gather upon NMO application and by the quality of mini stack panels.

The final velocity functions are listed in Appendix A for the four lines. In the regions where data quality was good and confident picks could be made it was quite common for the stacking velocity to be higher than 6000 m/s by 1 s two-way time. In regions of steep dip, for example on the southern end of line 97AGS-SD1, the stacking velocities are in excess of 7000 m/s, which are not representative of true rock velocities. At CDP 3700, stacking velocity is equal to 7500 m/s at 1.2 s. These high values can be explained by presence of layers dipping at 40° (in the plane of the section) and are consistent with the relationship for dipping events on a CDP gather, $V_{app} = V/\cos(\text{dip})$. (Note that the dip appears to be 33° on the unmigrated section and would convert to 40° upon migration). Dip moveout correction would be warranted prior to stack and migration in such areas, but is precluded by the low fold and crooked line.

3.10 Coherency Enhancement.

Coherency enhancement using the modules SIGNAL and DIGISTK was necessary on both shot records and CDP stack. The module SIGNAL is used for calculating the coherency of events for a range of specified dips, and outputs a set of SIGNAL traces, one for each input trace, which represents the coherent components of the original data. The DIGISTK module outputs traces which are a weighted linear combination of the data traces and the signal traces. A weight of zero reproduces the original data; a weight of one gives the coherence of the data and an intermediate value results in coherency-enhanced data.

Significant reduction in linear noise trains on the stack occurred as a result of limiting the dip range of the coherency operator on the moveout corrected shot records. Coherency enhancement was used also on CDP gathers, but was limited to the processing stream for calculating autostatics. In addition, coherency enhancement was necessary to improve the appearance of the CDP stack sections.

3.11 Stack

After NMO correction and application of a 20% stretch mute, the traces in each CDP gather were stacked to produce a single CDP trace using the alpha-trimmed mean option in the module MEDSTK. This employs a mixed mean and median technique so that at each sample time, the highest amplitude values and lowest value amplitudes are omitted from the stack according to a specified percentage of the total number of live traces. In this case 15% of values were dropped from each end of the amplitude range. The median stacking technique provides a better statistical estimate of the seismic signal when the background noise is non-Gaussian, ie, contains large amplitude values due to ground roll or other source-generated noise.

3.12 Migration

Migration tests were carried out on the stacked data using the finite difference algorithm employed by the module MIGRATX, with a range of migration velocity functions. Due to the poor continuity of seismic reflections and the limited windows of good data, there was not sufficient migration aperture for successful application. For this reason, the final stack sections were used for interpretation.

3.13 Additional processing tests on 97AGS-HB2

In view of the poor data on line 97AGS-HB2 in key areas, such as Mining Area 'C', an additional effort was made to improve the signal to noise ratio. F-K filtering was employed on the moveout corrected shot records, as well as coherency enhancement, but with no improvement. Experiments were done limiting the range of offsets in the stack to near offset only and far offsets only. In one test, traces recorded at stations known to be located in highly attenuating regolith were omitted from the stack.

After presentation of the final stacks for first pass interpretation, further processing was carried out on 97AGS-HB2, including tests to validate the original choice of spectral equalisation parameters. Because of the regolith problems in the key areas, the first break picks were reassessed, modified where necessary and run through the refraction statics analysis again. This necessitated updating the stacking velocity functions and recalculation of autostatics. Overall, the modifications were minor and did not result in any significant improvement.

4. ARCHIVAL

The SEG-Y shot ordered field data was value added by including additional information into the headers prior to writing to archive 3480 tapes. A sample EBCDIC header is presented in Appendix B, as well as a listing of the archive tapes. The main innovation was the introduction of a methodology for storing first break picks from the database in the SEG-Y trace headers. The final stacks were also archived in SEG-Y format on 3480 tapes. The EBCDIC header and listing of the stack archive tapes is also given in Appendix B.

5. PRELIMINARY INTERPRETATION

5.1 Reflection

The final stacks were displayed as variable density sections at 1:1 scale for each of the lines 97AGS-SD1, 97AGS-HB1, 97AGS-HB2 and 97AGS-HB3 (Figures 10 to 13 respectively). Overall, the final results are disappointing, with the good data confined to narrow areas or "windows".

In the deeper crustal sections (not shown) the appearance of good mid-crustal and deeper reflections in some regions of upper poor coherency indicate that the energy was penetrating the Hamersley Province but the reflective nature of the Hamersley sediments precluded good reflections. These areas are related to either near surface geological variations which have resulted in a significant shift in the frequency content of the signal towards the lower frequencies or to areas where the structure or lithology is not conducive to producing reflections.

Sylvania Dome Traverse (97AGS-SD1)

Data quality varied considerably. Good reflections were imaged in the northern third of the traverse, within the Fortescue Group, and in the southern third within the granite-greenstone terrane of the Sylvania Dome (Figure 10). However reflection strength and continuity within the middle section within the Hamersley Group were significantly reduced (Figure 10). Some of the lack of continuity could be due to problems imaging the complex structure in the region. The effect of regolith and sub-surface geology will be discussed later.

Of particular interest is the imaging of a series of southerly dipping series of reflections within the Sylvania Dome (Figure 10) overlying subhorizontal reflections. The marked change in dip at station 1750 is a geometric effect caused by a bend in the seismic line. In the upper part of the section between stations 1600 and 1800, an irregular dipping interface separates a reflection free zone from dipping reflectors beneath. This bland zone and its lower boundary are interpreted as the seismic expression of Archaean granite.

Hamersley Basin Line 1 (97AGS-HB1)

Of the three lines constituting the Hamersley Basin Traverse, by far the best is line 97AGS-HB1, where the northern third displays high quality reflections, within the relatively undeformed Hamersley Basin (Figure 11). In the upper 1.5 s between stations 1000 and 1200, a broad syncline comprising the Fortescue Group is apparent. Below this, the several packages of reflectors are presumably Archaean granite-greenstone terrane. However reflection strength and continuity within the middle section and in the southern section within the Hamersley Group are significantly reduced.

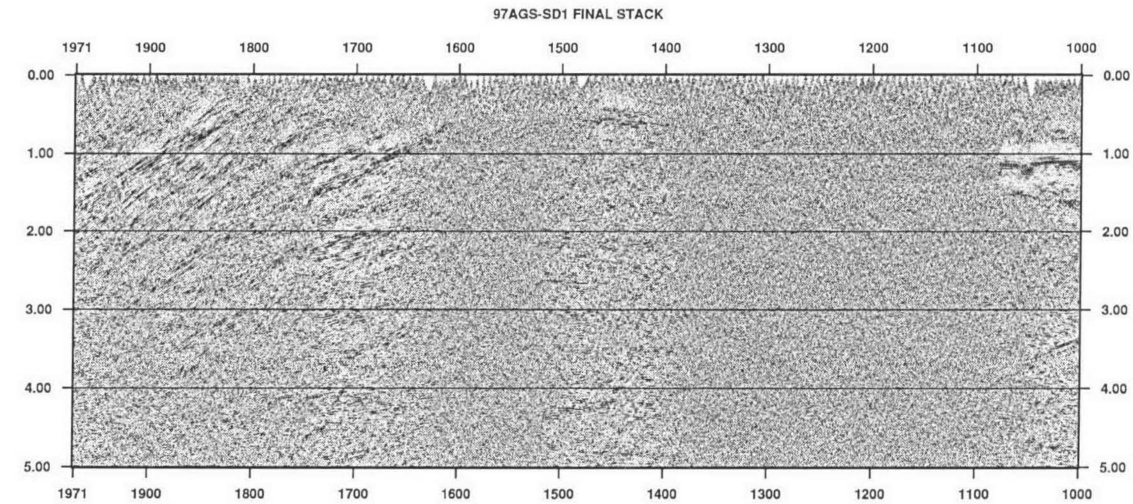

Figure 10: Final unmigrated stack for Hamersley line 97AGS-SD1 Station number is annotated on the distance axis (100 = 4 km). North is to the right. V/H=1 at 6000 m/s.

Hamersley Basin Line 2 (97AGS-HB2)

Data quality again varied considerably (Figure 12). Good reflections imaged within a window on the southern part of the line show a more highly deformed part of the Hamersley Province. The poor data areas can be explained by the problems encountered recording through the Marra Mamba Formation. The Marra Mamba is very cavernous and significant difficulty was encountered in getting sufficient seismic energy into the ground.

In the areas where the Marra Mamba was either cropping out or just below the surface ie, the area within Area 'C', the Weeli Wolli Anticline and near Coondawanda Hill and West Angelas, the reflection strength and continuity were reduced. Better reflections were imaged in the southern section of the traverse, just to the north of Mount Hilditch (Figure 12).

Hamersley Basin Line 3 (97AGS-HB3)

Data quality again varied considerably (Figure 13). Good reflections were imaged within the northern section of the line over the Wanna Munna Flats, within various windows along the traverse and in the southern section of the line within the Fortescue Group. However reflection strength and continuity within the middle section within the Hamersley Group were significantly reduced (Figure 13).

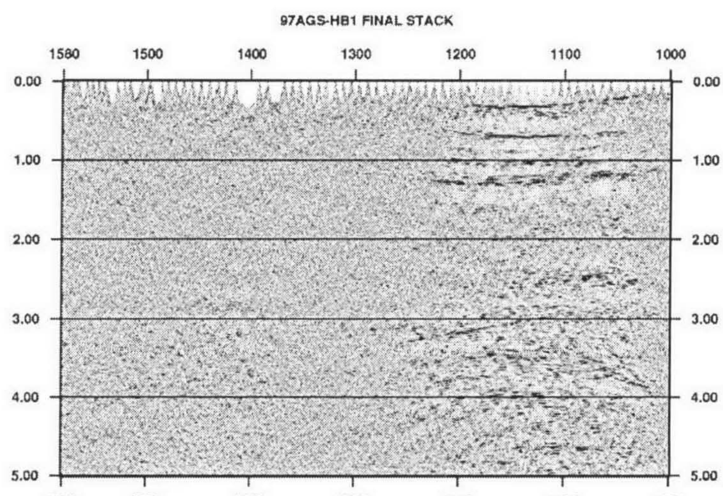

Figure 11: Final unmigrated stack for Hamersley line 97AGS-HB1 Station number is annotated on the distance axis (100 = 4 km). North is to the right. V/H=1 at 6000 m/s.

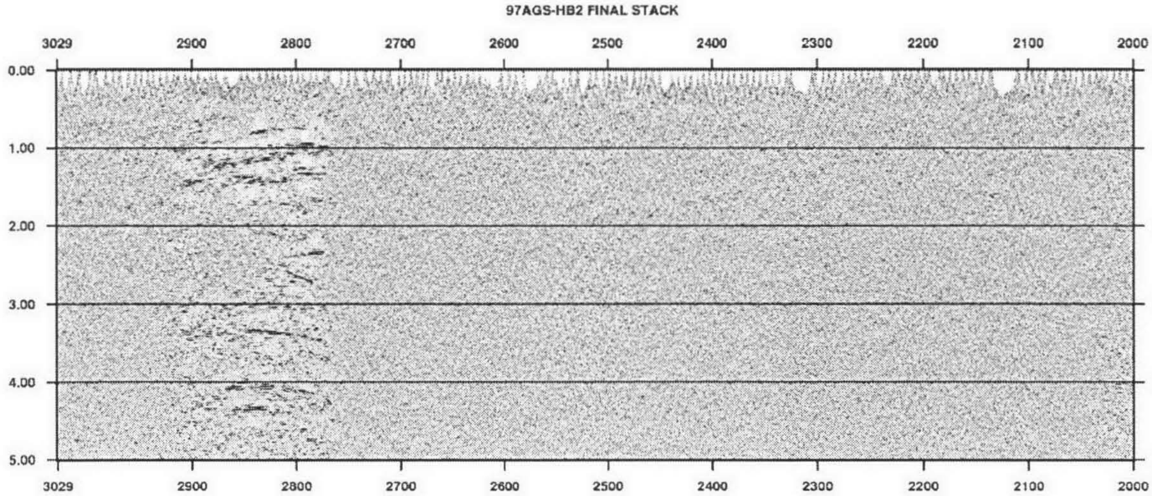

Figure 12: Final unmigrated stack for Hamersley line 97AGS-HB2. Station number is annotated on the distance axis (100 = 4 km). North is to the right. V/H=1 at 6000 m/s.

Discussion of seismic reflection data quality

The reduction in reflection amplitude and continuity in the poor data areas can be partly attributed to the structure within the region and partly to the problem of loss of seismic energy. The main reasons for the poor data quality was high absorption of the seismic signal by the Marra Mamba Formation (Hamersley Group) and problems with a weathered layer of variable thickness, overlain by gravels in the valleys. This type of regolith produced a significant shift in the frequency content of the signal towards the lower frequencies. In addition, at the large contrast in velocity at the base of regolith, a significant amount of the energy is critically refracted and reflected.

Fair to good quality seismic data were recorded wherever the traverse was located over a unit that was stratigraphically below the Marra Mamba or in regions other than that within the Hamersley Group. Good to excellent data was obtained from within the granitic Sylvania Dome, the Bresnahan Basin and the Fortescue Group region (Figure 1).

The relationship between thick regolith and lack of data on the seismic sections becomes more apparent upon examining the information plotted in Figure 14. For each of the lines, the delay time to the refractor (interpreted as the base of weathering) is plotted alongside the uphole time measured for the shot. Also shown on the plots is the extent of good and fair seismic reflection data, as evaluated on the seismic sections.

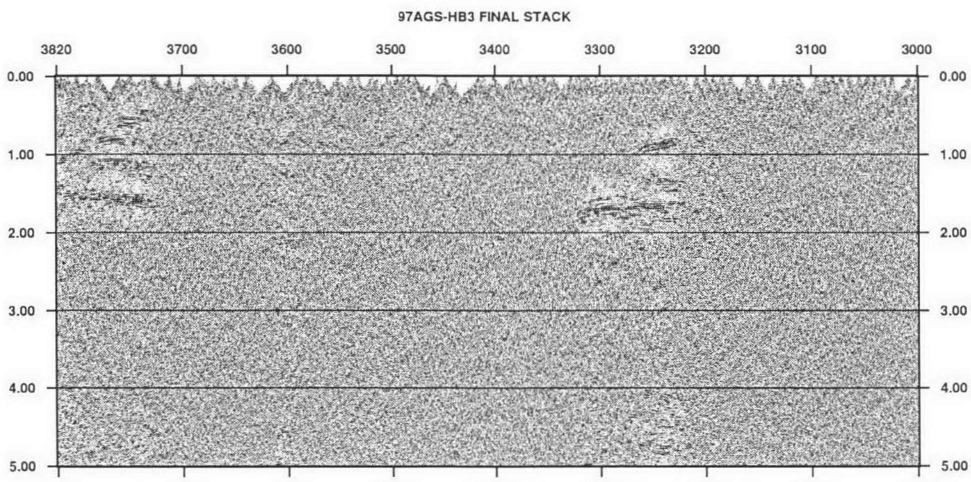

Figure 13: Final unmigrated stack for Hamersley line 97AGS-HB3. Station number is annotated on the distance axis (100 = 4 km). North is to the right. V/H=1 at 6000 m/s.

On lines 97AGS-HB2, 97AGS-HB3 and 97AGS-SD1, the areas of good data correspond to places where the uphole time is very close to the delay time – in other words, the shot is placed close to or below the base of weathering. These are obviously also areas where the weathering is least, as shown by the low delay times, and thus the shot hole can penetrate through the weathering. On the northern end of line 97AGS-HB1, the shots are not quite as close to the base of weathering, but the data quality is still good.

These areas of least weathering correspond closely to more resistant units identified by the mapped geology. For the Hamersley Basin Traverse, the good data windows lie within the Fortescue Group in the Jeerinah Formation, which has been intruded by dolerite sills. Along the Sylvania Dome Traverse, the good data window along the southern half of the line lies within Archaean granite. In areas of the deepest weathering, data quality is poor for all the lines. However, the explanation is a little more complicated than this, and other factors must be considered. In the intermediate areas, fair data is obtained with moderate thickness of weathering, provided that the shots and receivers are not located in the Marra Mamba Formation. In the middle of line 97AGS-SD1, the data quality is only fair, although the regolith does not appear to be very thick.

Although the seismic data are generally not good, some significant details are shown within areas of the Hamersley Province which provide sufficient information for development of a crustal structure model.

5.2 Shallow Refraction Results

Since a single refractor model was employed for calculation of refraction statics, it was not possible to distinguish between surficial deposits (gravels) and in-situ weathering profile. However, the refractor elevation and velocity profiles can provide additional information to assist in interpretation of the seismic reflection data. For example, the depth of weathering has already been demonstrated to be least in the Fortescue Group and the Sylvania Dome Granite.

On several of the lines (eg 97AGS-HB2), pronounced lows occur in the refractor elevation, that is, weathering is more intense (Figure 6). These features appear to run along geological strike, as they can be correlated across the overlap from one line to the next in the Hamersley Basin. Several of these lows in refractor elevation also correspond to lows in refractor velocity, e.g. around station 3200 on line 97AGS-HB3 (Figure 7), and stations 2090 and 2680 on line 97AGS-HB2 (Figure 6). Two possible explanations for these lows are; (a) presence of faults which have facilitated weathering and caused a reduction in bedrock (refractor) velocity due to fracturing and (b) weathering controlled by steeply dipping units of the Marra Mamba Iron Formation the and Wittenoon Dolomite. A more sophisticated multi-layer refraction analysis would provide a better handle on near surface variations in velocity and structure, which could be related to sub-surface geology and in particular to the existence of faults.

6. DISCUSSION

The areas of poorest reflection data correspond to areas of deep weathering and valleys with alluvial gravels. Where weathering is apparently less a problem, it is the nature of the surficial geology that is responsible, for example the cavernous character of the Marra Mamba Formation.

For the reflection data, the biggest problem was getting the energy into the ground. Given the depth of weathering, it was not feasible to drill shot holes into unweathered rock. Tests were done drilling deeper holes (down to 58 m) and using larger charge sizes, but it was concluded that although the energy went into the ground, there was still the problem of dissipation of energy by the regolith on its return to the receivers.

It is recommended that surveys be carried out on units, which provide a good "window" into the sub-surface. In particular, the shots should be placed within these units, even if this involves non-standard spread configurations and undershooting. Source placement is even more critical for a surface source, although use of vibroseis technique would have the advantage of substantially increased fold and a major improvement in the signal to noise ratio.

To address some of the specific problems such as highly attenuating gravels, tests could be made with controlled seismic sources using a range of frequencies, to determine whether lower frequencies would be attenuated less. There would also be the opportunity to stack several sweeps at the same location. Another option with several controlled sources could be to steer a beam of energy into the ground, to counteract the fact that most of the energy is critically refracted and reflected at the large contrast in velocity at the base of weathering. Extensive modelling tests would be necessary to determine if this idea is feasible. It is worth bearing in mind that explosive sources are often superior to surface vibratory sources over unconsolidated gravels.

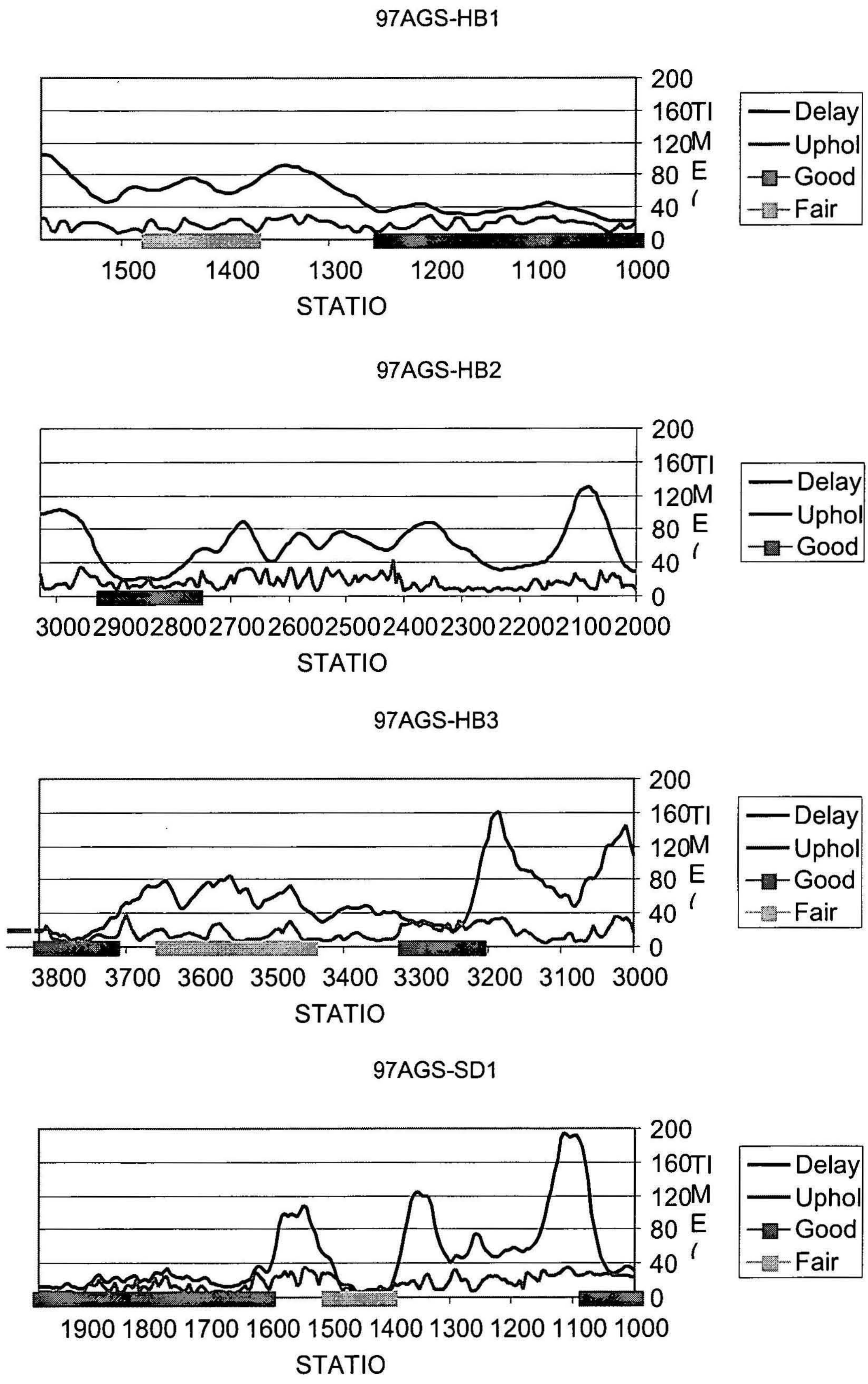

Figure 14: Comparison of time delay to refractor, shot uphole times and reflection data quality for (from top to bottom) 97AGS-HB1, 97AGS-HB2, 97AGS-HB3 and 97AGS-SD1. North is on the right to be consistent with the seismic sections.

An effort should also be made to improve the coupling of energy into the receivers in areas of unconsolidated material.

It would be worth investigating whether bunched geophones would have a better response than a linear geophone array, because of variable coupling along the array and consequent degradation of signal. In any case, a 40 m array is not effective at suppressing ground roll in these high velocity hardrock terrains, since the ground roll wavelength is greater than 100 m. It was shown earlier that spectral equalisation and filtering during processing was successful in suppressing ground roll.

7. ACKNOWLEDGMENTS

The authors publish with the permission of the Chief Executive Officer, Geoscience Australia. They wish to acknowledge the contribution of colleagues via discussions and suggestions. In particular, Joe Mifsud is thanked for drafting the geological map.

8. REFERENCES

Goleby, B.R., Barton, T.J. and Cherry, E.H., 2001. Hamersley Province Seismic Survey 1997: Operational Report. Geoscience Australia Record 2001/45, 23pp

Taner, M.T., Wagner, D.E., Baysal, E. & Lee, L., 1998. A unified method for 2-D and 3-D refraction statics. Geophysics, 63, 260–274.

APPENDIX A – STACKING VELOCITY FUNCTIONS

Time-Velocity functions listed for CDP's where velocity analysis was performed. Time is given in ms and velocity in m/s.

97AGS-SD1

2050		2100		2300		2500	
32	5462	20	5058	24	4605	24	4686
472	5476	460	5090	364	4589	332	4734
776	6061	872	5854	564	5478	612	4591
1088	6088	1188	6772	756	5495	2604	6691
1516	6950	1996	6934	1756	6190	3984	6869
2460	6918	3980	6999	2868	6222	20000	8000
3980	6999	20000	8000	3976	6578		
20000	8000			20000	8000		

2700		2900		3100		3250	
24	4912	24	4864	24	5915	24	4540
500	4905	288	4880	388	5850	180	4557
1008	5106	436	5884	756	4330	388	5608
1828	6174	568	5980	1372	6416	748	6711
2532	6513	1756	5640	1940	6643	1476	7063
3980	6643	2116	5689	3296	7063	2580	7496
20000	8000	3984	6530	3980	7128	3976	7516
		20000	8000	20000	8000	20000	8000

3400		3550		3700		3850	
24	4767	24	4589	20	4282	24	4896
256	4751	172	4589	168	4282	232	4880
620	6222	380	5333	548	7338	612	5721
1040	6804	908	7047	792	7338	900	6077
1348	6950	2072	7354	1216	7549	1388	7030
2060	7678	2988	7694	1676	7209	1728	7403
2312	7710	3980	7662	2244	7338	2240	7533
2672	7775	20000	8000	2620	7370	3136	7697
3056	7904			3256	7257	3976	7710
3992	7613			3992	7257	20000	8000
20000	8000			20000	8000		

97AGS-HB1

2100		2200		2300		2400	
28	5478	28	5495	24	5527	32	5042
220	5511	300	5495	300	5490	324	5042
656	6151	696	6475	696	5973	676	6362
1260	5817	1204	6594	1020	6125	976	6444
1816	5862	2032	6449	1904	5931	1292	6837
2476	5700	2772	6691	2892	6093	3204	6643
3024	5761	3976	6610	3404	6077	3980	6756
3612	6534	20000	8000	3980	6303	20000	8000
3984	6610			20000	8000		
20000	8000						

2500		2600		2750		2950	
24	5138	28	4168	24	4864	24	4831
284	5074	276	4201	512	4880	228	4831
656	5300	532	4621	820	5430	408	5239
1064	5398	848	5203	2424	6335	928	6334
1412	5980	1252	5668	3976	6675	1536	6416
2012	6610	2140	6360	20000	8000	2916	6853
3092	7051	3060	6821			3548	6999
3756	7327	3976	6950			3972	7047
3980	7273	20000	8000			20000	8000
20000	8000						

97AGS-HB2

4100		4200		4300		4400	
20	4896	36	4799	20	5753	24	5284
340	4912	184	4799	276	5721	608	5349
588	5381	444	4896	560	6578	988	5802
1692	6222	1352	6287	868	6465	1584	6513
3980	6918	1984	6707	1408	6659	3320	6918
20000	8000	3496	6982	2508	6821	3976	7039
		3984	7031	3976	6999	20000	8000
		20000	8000	20000	8000		

4500		4600		4700		4800	
36	5139	32	4831	32	5398	32	5381
460	5155	496	4896	616	5381	448	5381
1100	6012	732	5369	980	5915	1404	6271
2000	6772	1552	6433	1308	6303	2060	6902
3076	6932	2224	6627	1988	6821	2836	6902
3976	7031	3980	6982	3972	6999	3980	6999
20000	8000	20000	8000	20000	8000	20000	8000

4900		5000		5190		5400	
32	5058	20	5106	44	4977	24	5090
380	5042	392	5058	448	5009	464	5090
564	5495	916	6012	1236	6012	1096	5671
760	5559	1560	6659	1632	6287	1924	6675
1196	5980	3984	6999	2672	6902	3016	6966
1884	6497	20000	8000	3972	6999	3968	6999
2472	6966			20000	8000	20000	8000
3984	7015						
20000	8000						

5600		5700		5800		5950	
28	5802	20	5300	24	5624	24	5781
440	5817	480	5284	196	5608	400	5786
676	5866	832	5753	360	6303	940	6391
1228	6442	1260	6643	556	6636	1600	6497
1712	6271	3344	6950	796	6853	2352	6590
2128	6384	3980	6999	1456	6837	3984	6999
2672	6885	20000	8000	2976	6934	20000	8000
3980	6999			3984	6999		
20000	8000			20000	8000		

97AGS-HB3

6081		6181		6381		6581	
0	4000	0	4000	0	4000	0	6000
2300	6250	300	5000	300	5000	500	6500
4000	6500	800	5500	850	5500	1550	6500
20000	8000	2000	6000	1700	6000	4000	6500
		2400	6000	2050	6250	20000	8000
		4000	6500	4000	6500		
		20000	8000	20000	8000		

6866		7000		7150		7350	
0	5000	0	4000	0	5000	0	6000
800	5500	450	4500	500	6000	800	6500
1950	6000	800	5000	1000	6500	1200	6500
3000	6250	1100	5500	2250	6500	4000	6500
4000	6500	2500	6000	4000	6500	20000	8000
20000	8000	4000	6500	20000	8000		
		20000	8000				

7450		7550	
0	6000	0	6500
500	6000	4000	6500
1000	6500	20000	8000
1700	6500		
4000	6500		
20000	8000		

APPENDIX B – ARCHIVE TAPE DETAILS

Table B1: Sample listing of EBCDIC header for shots archived in SEG-Y format on 3480 tape.

```
C 1   AGSO ARCHIVAL 3480 TAPE (SEGY STANDARD): 'RAW' SHOT RECORDS (20 SEC 2 MS)
C 2   LINE      : 97AGS-SD1, SYLVANIA DOME
C 3   SURVEY    : L144, HAMERSLEY BASIN, WESTERN AUSTRALIA 1997
C 4   RECORDED : JULY - AUGUST 1997
C 5   STATIONS : 1000-1971 (N->S),  CDPS: 2000-3942, NO. SHOTS: 163
C 6   RECORDING DETAILS
C 7   SYSTEM TYPE    : SERCEL SN368,  NO. CHANNELS: 120
C 8   RECORDED ON 9-TRACK TAPE (SEGD 6250) & EXABYTE (SEGY TAR 8500)
C 9   ORIGINAL 9-TRACK FIELD TAPE NUMBERS 97/023 - 97/033
C10   RECORD LENGTH  : 20 SEC   SAMPLE RATE  : 2 MSEC
C11   RECORDING FILTERS  : LCF    -    8 HZ, 18 DB/OCT
C12                      : HCF (ALIAS)  - 178 HZ : NOTCH - OUT
C13   SOURCE TYPE     : POWERGEL (ICI),   DRILLS : MAYHEW 1000 (X 5)
C14   CHARGE          : 10 KG  (NOMINAL), DEPTH   : 36 M  (NOMINAL)
C15   SP INTERVAL     : 240.0 M  GROUP INTERVAL : 40.0 M
C16   CHANNEL NUMBER :  S 120        61        1 N
C17   SPREAD PATTERN :    2400 M -- 0 -- 2400 M
C18   GROUP PATTERN  :  16 IN-LINE, 2.5 M SPACING
C19   SHOT ON TRACE  :  61 (NOMINAL)
C20   COVERAGE        : 1000% (NOMINAL)
C21   CAB POSITION    : 1080,1242,1379,1460,1625,1729,1838,1855
C22   PROCESSING DETAILS
C23   1. GEOMETRY DEFINITION
C24   2. "MISFIRE" SHOTS (9,106,161) ZEROED ON ALL TRACES
C25   3. SHORT RECORD SHOTS (3,26,99,118,130,136,139,141,155) NOTED - NOT EDITED
C26   4. REFRACTION STATICS (REFSOL) PUT IN HEADER (INT & FP), BUT NOT APPLIED
C27   5. SORTED INTO SHOT ORDER
C28   6. HEADER INFORMATION ADDED (INC. CDP-X, CDP-Y & FIRST BREAKS)
C29   7. OUTPUT DATA TO AGSO ARCHIVAL 3480 TAPE IN SEGY FORMAT VIA DISCO/GOUT
C30   EXTRA HEADER ENTRIES (BYTES)
C31     189-190: 'SHOT'  SHOT NUMBER (MUST DEFINE IN DISCO/GIN)
C32     191-194: 'CDP-X' CDP-X COORDINATE
C33     195-198: 'CDP-Y' CDP-Y COORDINATE
C34     217-220: 'SHT-RFST' SHOT STATIC (FLOATING POINT VERSION OF 'SHSTAT')
C35     221-224: 'REC-RFST' RCVR STATIC (FLOATING POINT VERSION OF 'RCSTAT')
C36     225-226: 'FBPICK'   FIRST BREAK PICK (PEAK) IN MSEC (-1=NONE)
C37   PROCESSED BY: LAND SEISMIC GROUP, AGSO, GPO BOX 378, CANBERRA, ACT 2601
C38   GEOPHYSICISTS: BRUCE GOLEBY & LEONIE JONES  DATE : JANUARY 1999
C39   FOR FURTHER INFORMATION SEE OPERATIONS REPORT AGSO RECORD xx/xx
C40   COPYRIGHT RESERVED BY COMMONWEALTH OF AUSTRALIA, 1997.
```

Table B2: Listing of SEG-Y shot-ordered archive 3480 tapes, 20 s @ 2ms

TAPE #	LINE	SHOT (SEQNO)	SHOT (SEQNO)	SP	SP
		first	last	first	last
L14499053	97AGS-SD1	1 (1)	47 (46)	1000	1275
L14499054	97AGS-SD1	47 (47)	93 (57)	1275	1552
L14499055	97AGS-SD1	93 (58)	139 (18)	1552	1828
L14499056	97AGS-SD1	139 (19)	163 (120)	1828	1971
L14499057	97AGS-HB1	1 (1)	47 (57)	1000	1368
L14499058	97AGS-HB1	47 (58)	78 (120)	1368	1580
L14499059	97AGS-HB2	1 (1)	47 (45)	2000	2275
L14499060	97AGS-HB2	47 (46)	93 (82)	2275	2552
L14499061	97AGS-HB2	93 (83)	139 (113)	2552	2828
L14499062	97AGS-HB2	139 (114)	170 (120)	2828	3029
L14499063	97AGS-HB3	1 (1)	46 (115)	3000	3361
L14499064	97AGS-HB3	46 (116)	93 (19)	3361	3791
L14499065	97AGS-HB3	93 (20)	97 (120)	3791	3820

Table B3: Sample listing of EBCDIC header for stacked data archived in SEG-Y format on 3480 tape.

```
C 1 AGSO ARCHIVAL 3480 TAPE (SEGY STANDARD): STACKED DATA (20 SEC 4 MS)
C 2  LINE       : 97AGS-SD1, SYLVANIA DOME
C 3  SURVEY     : L144, HAMERSLEY BASIN, WESTERN AUSTRALIA, JULY-AUGUST 1997
C 4  STATIONS  : 1000-1971 (N->S);  CDPS: 2000-3942; NO. SHOTS: 163
C 5  ORIGINAL 9-TRACK FIELD TAPE NUMBERS 97/023 - 97/033
C 6  RECORDING FILTERS: LCF - 8 HZ, 18 DB/OCT; HCF - 178 HZ; NOTCH - OUT
C 7  SOURCE TYPE      : POWERGEL (ICI), 10 KG (NOMINAL), 36 M DEPTH (NOMINAL)
C 8  SP INTERVAL - 240.0 M; GROUP INTERVAL - 40.0 M; CDP INTERVAL - 20.0 M
C 9  SPREAD PATTERN : 120 CHANNELS, SPLIT SPREAD, SHOT AT 61 (NOMINAL)
C10  COVERAGE     : 1000% (NOMINAL)
C11  PROCESSING DETAILS
C12  1. DEMULTIPLEX: SEGD TO SEGY USING FIELD EAVESDROPPER SYSTEM
C13  2. GEOMETRY DEFINITION
C14  3. RESAMPLE DATA TO 4 MS
C15  4. "MISFIRE" SHOTS (9,106,161) ZEROED ON ALL TRACES
C16  5. SHORT RECORD SHOTS (3,26,99,118,130,136,139,141,155) ENDMUTED
C17  6. NOTCH FILTER APPLIED AT CAB POSITIONS (& PREVIOUS & NEXT STATION)
C18  7. SPHERICAL DIVERGENCE CORRECTION C=1.0,V=2.0,T=1.0, VELOCITY 5-8 KM/S
C19  8. SPECTRAL EQUALISATION INPUT GATES: (8/12-16/20) X 8
C20     OUTPUT GATE WEIGHTS : 0/0, 8/0.5, 16/1, 24/1.5, 0/2,64/1.5,72/0.5,100/0
C21  9. BANDPASS FILTER  TIME (SEC)   BANDPASS(HZ)/SLOPE(DB/OCTAVE)
C22                       0.0           24/36 - 72/36
C23                       4.0           20/36 - 72/36
C24                      20.0           12/36 - 40/36
C25  10. MUTE APPLIED (ON INDIVIDUAL SHOTS) AFTER SPEQ AND BP FILTER
C26  11. REFRACTION STATICS; DATUM 440 M; REPLACEMENT VELOCITY 5.6 KM/S
C27  12. AUTOSTATICS WITH STRUCTURE
C28  13. SHOT BALANCE
C29  14. NORMAL MOVEOUT CORRECTION (20% STRETCH MUTE)
C30  15. COHERENCY ENHANCEMENT - SHOTS (SIGNAL & DIGISTK)
C31  16. CDP SORT (TO CROOKED LINE)
C32  17. MEDIAN STACK
C33  18. SECTION BALANCE
C34  19. COHERENCY ENHANCEMENT - CDP SECTION (SIGNAL & DIGISTK)
C35  20. AGC - 500 MS GATE
C36  21. EXTRA HEADER ENTRIES ('CDP-X',191-194 BYTES;'CDP-Y',195-198 BYTES)
C37 PROCESSED BY: LAND SEISMIC GROUP, AGSO, GPO BOX 378, CANBERRA, ACT 2601
C38 GEOPHYSICISTS: BRUCE GOLEBY & LEONIE JONES,  DATE: JANUARY 1999
C39 FOR FURTHER INFORMATION SEE PROCESSING REPORT AGSO RECORD xx/xx
C40 COPYRIGHT RESERVED BY COMMONWEALTH OF AUSTRALIA, 1999.
```

Table B4: Listing of SEG-Y stack archive 3480 tapes, 20 s @ 4 ms

TAPE #	LINE	CDP	CDP
		first	last
L14499066	97AGS-SD1	2000	3942
L14499067	97AGS-HB1	2000	3160
L14499068	97AGS-HB2	4000	6058
L14499069	97AGS-HB3	6000	7640